Cellular Microbiology (2013) **15**(12), 2093–2108
doi:10.1111/cmi.12175
First published online 22 August 2013

# Mannan core branching of lipo(arabino)mannan is required for mycobacterial virulence in the context of innate immunity

**Esther J. M. Stoop,[1†] Arun K. Mishra,[2†] Nicole N. Driessen,[1] Gunny van Stempvoort,[1] Pascale Bouchier,[1] Theo Verboom,[1] Lisanne M. van Leeuwen,[1] Marion Sparrius,[1] Susanne A. Raadsen,[1] Maaike van Zon,[3] Nicole N. van der Wel,[3] Gurdyal S. Besra,[4] Jeroen Geurtsen,[1] Wilbert Bitter,[1,5] Ben J. Appelmelk[1] and Astrid M. van der Sar[1*]**

[1]*Department of Medical Microbiology and Infection Control, VU University Medical Center, van der Boechorststraat 7, 1081 BT Amsterdam, The Netherlands.*

[2]*Mycobacterial Research Division, National Institute for Medical Research, The Ridgeway, Mill Hill, London, NW7 1AA, UK.*

[3]*Division of Cell Biology-B6, Netherlands Cancer Institute-Antoni van Leeuwenhoek Hospital (NKI-AVL), 1066 CS Amsterdam, The Netherlands.*

[4]*School of Biosciences, University of Birmingham, Edgbaston, Birmingham, B15 2TT, UK.*

[5]*Department of Molecular Microbiology, VU University, de Boelelaan 1085, 1081 HV Amsterdam, The Netherlands.*

## Summary

**The causative agent of tuberculosis (TB), *Mycobacterium tuberculosis*, remains an important worldwide health threat. Although TB is one of the oldest infectious diseases of man, a detailed understanding of the mycobacterial mechanisms underlying pathogenesis remains elusive. Here, we studied the role of the α(1→2) mannosyltransferase MptC in mycobacterial virulence, using the *Mycobacterium marinum* zebrafish infection model. Like its *M. tuberculosis* orthologue, disruption of *M. marinum mptC* (mmar_3225) results in defective elongation of mannose caps of lipoarabinomannan (LAM) and absence of α(1→2) mannose branches on the lipomannan (LM) and LAM mannan core, as determined by biochemical analysis (NMR and GC-MS) and immunoblotting. We found that the *M. marinum mptC* mutant is strongly attenuated in embryonic zebrafish, which rely solely on innate immunity, whereas minor virulence defects were observed in adult zebrafish. Strikingly, complementation with the *Mycobacterium smegmatis mptC* orthologue, which restored mannan core branching but not cap elongation, was sufficient to fully complement the virulence defect of the *mptC* mutant in embryos. Altogether our data demonstrate that not LAM capping, but mannan core branching of LM/LAM plays an important role in mycobacterial pathogenesis in the context of innate immunity.**

Received 25 February, 2013; revised 3 July, 2013; accepted 17 July, 2013. *For correspondence. E-mail a.vandersar@vumc.nl; Tel. (+31) 20 44 48296; Fax (+31) 20 44 48318.
†These authors contributed equally to this work.



## Introduction

*Mycobacterium tuberculosis*, the causative agent of tuberculosis (TB), is a successful pathogen which has infected approximately one-third of the world's population (Dye *et al.*, 1999). Although a comprehensive picture of mycobacterial factors required for pathogenesis still remains, an essential role for the mycobacterial cell wall has been suggested (Karakousis *et al.*, 2004). The lipid rich cell envelope serves as a template for glycoconjugates, such as phosphatidyl-*myo*-inositol mannosides (PIMs), lipomannan (LM) and lipoarabinomannan (LAM) (Briken *et al.*, 2004; Mishra *et al.*, 2011a). PIMs are composed of a mannosylphosphatidyl-*myo*-inositol (MPI) anchor substituted with one to five mannose residues ($PIM_1$ to $PIM_6$). Additionally, the MPI moiety can be further covalently linked to an α(1→6)-mannopyranose (man*p*) core decorated by singular α(1→2)-man*p* branching units to form LM (Chatterjee *et al.*, 1993; Mishra *et al.*, 2011a). LM probably serves as a precursor of LAM that is further glycosylated by arabinan residues leading to a highly branched arabinan domain (Birch *et al.*, 2010; Alderwick *et al.*, 2011) (Fig. S1). LAM molecules can be classified into three distinct classes, based on the structural differences of the capping motifs present on the arabinan domain. LAM can be devoid of any capping motif, resulting in AraLAM such as in *Mycobacterium chelonae*

(Guerardel *et al*., 2002), capped by phosphoinositol (PI) units leading to PILAM as found in *Mycobacterium smegmatis* (Khoo *et al*., 1995), or further modified by man*p* capping units resulting in ManLAM as is the case in *M. tuberculosis* and *Mycobacterium marinum* (Appelmelk *et al*., 2008; Kaur *et al*., 2008). Mannose caps of ManLAM vary in length and consist of a single $\alpha(1\rightarrow5)$-man*p* that can be elongated with one or two $\alpha(1\rightarrow2)$-man*p* units (Besra *et al*., 1997; Nigou *et al*., 2003) (Fig. S1).

Since ManLAM is found almost exclusively in slow-growing mycobacterial species, which include most pathogens (Nigou *et al*., 1997; Khoo *et al*., 2001; Guerardel *et al*., 2003; N.N. Driessen *et al*., in preparation), it has been hypothesized that mannose caps on LAM are important for mycobacterial virulence. Indeed, it has been demonstrated that ManLAM is involved in inhibition of phagosomal maturation (Fratti *et al*., 2003; Vergne *et al*., 2003; Hmama *et al*., 2004; Kang *et al*., 2005) and in modulation of cytokine-mediated mechanisms of host resistance (Sibley *et al*., 1988; Chan *et al*., 1991; Knutson *et al*., 1998; Nigou *et al*., 2001; Pathak *et al*., 2005). Additionally, ManLAM is a ligand of the dendritic cell (DC)-specific intracellular adhesion molecule-3-grabbing non-integrin (DC-SIGN), and via this interaction it induces production of the anti-inflammatory cytokine IL-10 (Geijtenbeek *et al*., 2003; Maeda *et al*., 2003; Tailleux *et al*., 2003; Wu *et al*., 2011). However, the above mentioned studies were performed with purified LAM preparations. Studies using isogenic mycobacterial mutants defective for the $\alpha(1\rightarrow5)$ mannosyltransferase essential for mannose capping indicated that ManLAM does not dominate host–pathogen interactions (Appelmelk *et al*., 2008; Festjens *et al*., 2011; Afonso-Barroso *et al*., 2012), stressing the fact that such studies need to be done using the whole bacterium instead of purified material.

Apart from capping motifs of LAM, the mannan core of LAM and LM has also been implicated in virulence. LM from *M. tuberculosis*, which is generally longer, more branched and has a less acylated MPI anchor than *M. smegmatis* LM, inhibits host immune signalling, whereas the *M. smegmatis* variant does not (Rajaram *et al*., 2011; Torrelles *et al*., 2011). Furthermore, LM can activate pro-inflammatory immune responses via interaction with Toll-like receptor-2 (TLR-2) (Jones *et al*., 2001; Vignal *et al*., 2003; Dao *et al*., 2004; Quesniaux *et al*., 2004; Nigou *et al*., 2008; Mishra *et al*., 2011b) and potency depends on the same structural characteristics as described for interspecies variation (Nigou *et al*., 2008; Rajaram *et al*., 2011). Interestingly, a mutated mycobacterial LAM with a truncated arabinan domain exhibited an increased TLR-2-dependent pro-inflammatory activity, which indicates that the arabinan moiety of LAM covers the LM structure, thereby blocking its immunostimulatory effects (Birch *et al*., 2010). Furthermore, using LAM and a hypermannosylated mutant LM from *Corynebacterium glutamicum*, we observed that these heterogenous molecules are recognized by dendritic cells, mainly via TLR-2, and that mutant LM induces stronger *in vitro* and *in vivo* cytokine responses (Mishra *et al*., 2012).

The *M. marinum* zebrafish infection model has become a popular model to study mycobacterial pathogenesis. *M. marinum* is a close genetic relative of *M. tuberculosis* (Stinear *et al*., 2008) and in its natural hosts, ectotherms, it causes a TB-like disease. This disease is characterized by the formation of granulomas; organized aggregates of (infected) macrophages, surrounded by lymphocytes and fibroblasts (Ramakrishnan *et al*., 1997; Talaat *et al*., 1998; Prouty *et al*., 2003; van der Sar *et al*., 2004; Swaim *et al*., 2006; Broussard and Ennis, 2007). Whereas formation of granulomas used to be regarded as a host-driven process, there is a growing appreciation of an active role of the bacterium in the granuloma response. In transparent zebrafish embryos that possess only an innate immune system, it has been shown that *M. marinum* promotes the formation of cellular aggregates that recapitulate host and bacterial cell properties of adult granulomas (Davis *et al*., 2002; Volkman *et al*., 2004; Stoop *et al*., 2011). Using the *M. marinum* zebrafish embryo model, we recently performed a forward genetic screen to identify mycobacterial genes involved in granuloma formation and virulence (Stoop *et al*., 2011). For this, we infected zebrafish embryos with individual *M. marinum* transposon mutants and selected for mutants that were attenuated for bacterial aggregation as compared with wildtype. In the present work, we further characterized one of these early granuloma mutants, which is disrupted in gene *mmar_3225*. The *M. tuberculosis* orthologue of this gene, *Rv2181*, encodes an $\alpha(1\rightarrow2)$ mannosyltransferase (*mptC*) involved in the addition of the mannose branches on the mannan core of LM and LAM and elongation of the mannose caps on the arabinan domain of LAM (Kaur *et al*., 2008; Sena *et al*., 2010; Mishra *et al*., 2011b). We have demonstrated that the *M. marinum mptC* and its *M. tuberculosis* orthologue are functionally conserved and involved in virulence in zebrafish embryos. By complementation studies we were able to separate the dual role of the gene and established that not the length of the mannose caps of LAM, but the presence of mannose branching of the mannan core of LM and/or LAM is important for mycobacterial virulence in the context of innate immunity.

## Results

### *Identification of a* M. marinum *mptC mutant*

We analysed 1000 mutants from a random transposon mutant library of the fluorescently labelled *M. marinum*

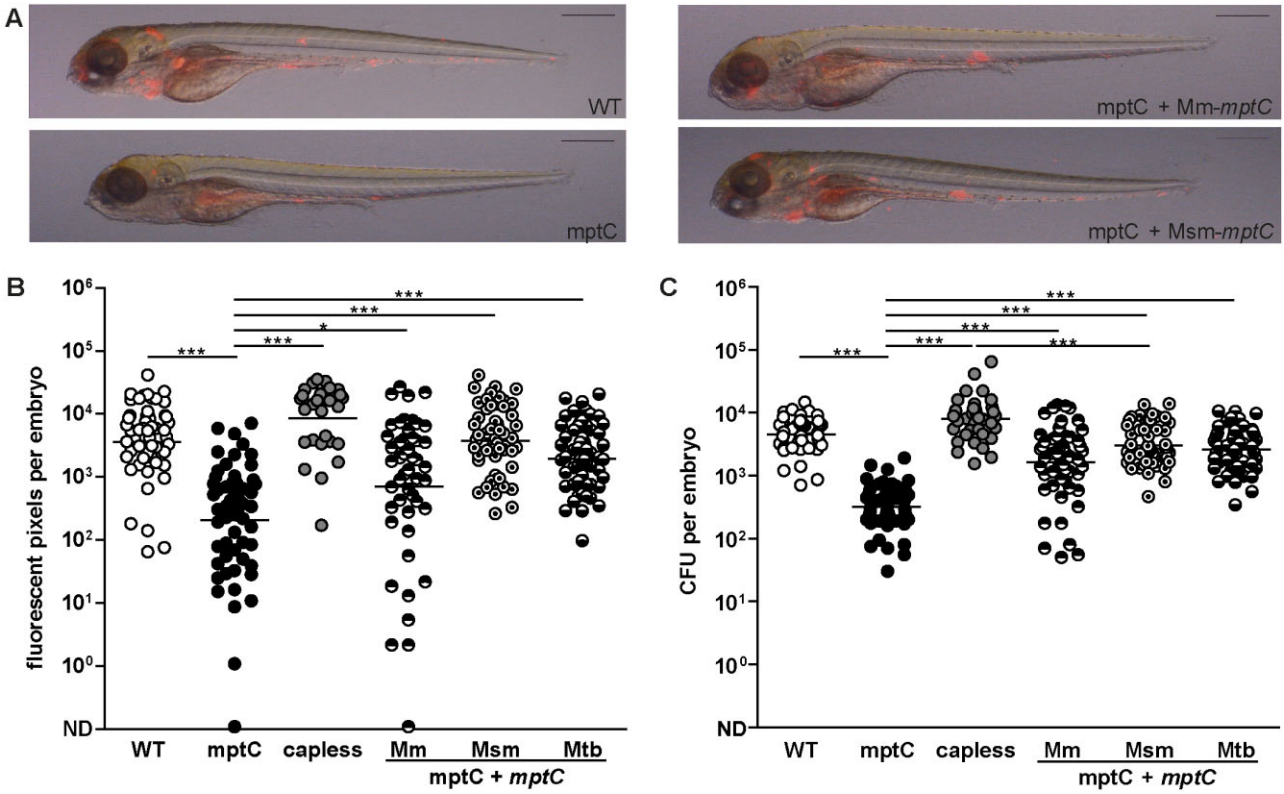


**Fig. 1.** Transposon mutant in *mmar_3225* attenuated for granuloma formation in zebrafish embryo model.
A. Representative overlays of brightfield and fluorescent images of embryos at 5 dpi with wildtype *M. marinum* (WT), *mptC* mutant (mptC), *mptC* mutant complemented with *M. marinum mptC* (mptC + *mptC* Mm) and *mptC* mutant complemented with *M. smegmatis mptC* (mptC + *mptC* Msm). Inocula were 117, 158, 138, and 198 cfu respectively. Scale bars represent 500 μm.
B and C. Quantification of embryo infection at 5 dpi with wildtype *M. marinum*, the *mptC* mutant, the capless mutant (capless), the *mptC* mutant complemented with *M. marinum mptC*, the *mptC* mutant complemented with *M. smegmatis mptC* and the *mptC* mutant complemented with *M. tuberculosis mptC* (mptC + *mptC* Mtb). (B) Number of red pixels in fluorescent images of infected embryos as determined with custom-designed software and (C) number of cfu of single infected embryos as determined by whole-embryo plating. Both graphs show data of three independent experiments and the bars represent mean after log transformation. Mean ± standard deviation of inocula were 99 ± 6, 149 ± 9, 99 ± 6, 134 ± 18, 144 ± 21 and 104 ± 13 cfu respectively. $*P < 0.05$, $***P < 0.0001$, one-way ANOVA, Bonferroni's multiple comparison test on log transformed data. ND, not detected.

E11 strain (Mma11) and screened for mutants with reduced initiation of granuloma formation in embryonic zebrafish. Upon intravenous injection of 50–200 colony-forming units (cfu) of wildtype *M. marinum* at 1 day post fertilization (dpf), aggregates of intracellular bacteria are observed at 5 days post infection (dpi) (Fig. 1A). Although adaptive immunity is not developed at this stage, it has been shown that these aggregates share both histological characteristics and gene expression profiles with adult granulomas (Davis *et al*., 2002; Stoop *et al*., 2011) and therefore, we refer to them as early granulomas. The screen led to the identification of 23 mutants that showed impaired early granuloma formation (E.J.M. Stoop *et al*., in preparation). In one of the mutants, FAM223, the transposon inserted 286 nucleotides downstream of the start codon of gene *mmar_3225*, the orthologue of the *M. tuberculosis* gene *Rv2181* (71% identical at the protein level). *Rv2181* encodes an α(1→2) mannosyltransferase (MptC) required for mannose branching of the mannan backbone of both LM and LAM and extension of the mannose caps of LAM (Kaur *et al*., 2006; 2008; Sena *et al*., 2010; Mishra *et al*., 2011b). From here on we will refer to mutant FAM223 as *mptC* mutant.

Bacterial aggregate formation of the *mptC* mutant was severely affected at 5 dpi (Fig. 1A). Quantification of infection was performed using two independent methods. First, customized software was used to determine the number of red pixels in fluorescent images of infected embryos (Stoop *et al*., 2011). This analysis showed that the infection level of the *mptC* mutant was 17-fold reduced as compared with wildtype *M. marinum* (Fig. 1B). In addition, we determined bacterial loads per embryo by plating infected embryos (Fig. 1C). Almost identical attenuation levels were observed with the two methods, as the mean bacterial load of embryos infected with the *mptC* mutant was 14-fold lower than that of the wildtype. These results

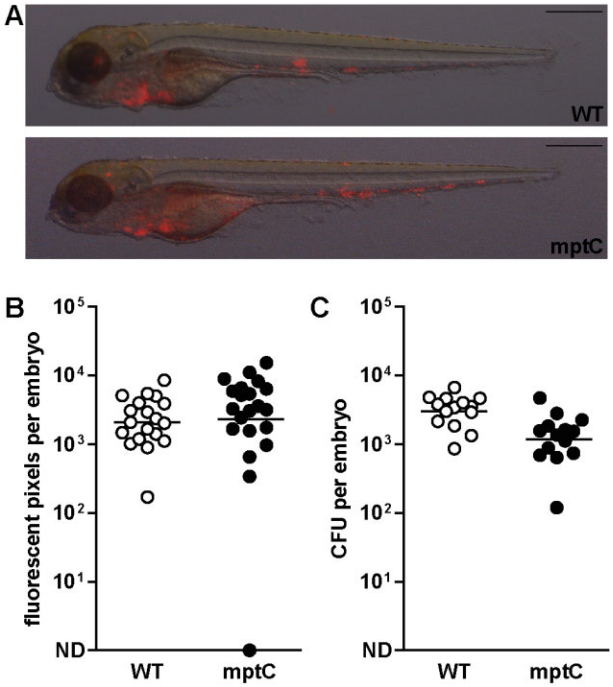


**Fig. 2.** High *mptC* mutant inoculum restores attenuated virulence in zebrafish embryos.
A. Representative overlays of bright field and fluorescent images of embryos at 5 dpi with wildtype *M. marinum* (WT) or *mptC* mutant (mptC). Scale bars represent 500 μm.
B. Number of red pixels in fluorescent images of infected embryos as determined with custom-designed software and (C) number of cfu of single infected embryos as determined by whole-embryo plating. Both graphs show data of two independent experiments and the bars represent mean after log transformation.
Mean ± standard deviation of inocula were 175 ± 81 and 419 ± 108 cfu respectively. ND, not detected.

demonstrate that MptC is involved in virulence and bacterial replication in zebrafish embryos.

To exclude that the *mptC* mutant is intrinsically impaired for growth *in vivo*, we analysed if higher inocula could revert the attenuated virulence phenotype to wildtype. Indeed, we observed similar levels of infection and bacterial aggregation with the *mptC* mutant and the wildtype *M. marinum* when 2.4-fold more *mptC* mutant than wildtype bacteria were used (Fig. 2). These results indicate that the *mptC* mutant can replicate *in vivo* and that more *mptC* mutant than wildtype bacteria are required for bacterial aggregation to occur, suggesting a specific function for MptC in virulence.

### *Complementation of the* M. marinum *mptC mutant*

To demonstrate that the mutant phenotype was caused by the transposon insertion, we reintroduced the wildtype *M. marinum mptC* in the *mptC* mutant using a mycobacterial integrative plasmid and examined the phenotype of this complemented mutant in zebrafish embryos. In response to infection with the complemented mutant, bacterial aggregation and bacterial replication *in vivo* were largely restored (Fig. 1A–C).

Furthermore, we analysed the ability of the *M. tuberculosis mptC* to restore the phenotype of the *mptC* mutant. Upon expression of *M. tuberculosis mptC*, restoration of the mutant phenotype was comparable with that of the *mptC* mutant complemented with the *M. marinum mptC*, both in terms of bacterial aggregation and replication (Fig. 1B and C). Thus, *M. marinum mptC* and its *M. tuberculosis* orthologue are functionally conserved.

### *Characterization of LM and LAM of the* M. marinum *mptC mutant with specific antibodies and lectins*

Wildtype *M. marinum* and the *mptC* mutant exhibited identical growth characteristics on solid medium as well as in liquid culture (data not shown). In addition, susceptibility to antibiotics (streptomycin, erythromycin, isoniazid, rifampicin, polymyxin B and chloramphenicol) (Table S1) and protein profiles (data not shown) of the mutant were similar as those of the parent strain, indicating that the attenuated phenotype was not the result of a growth defect or a gross change in cell wall integrity.

Because it has been described that the *M. tuberculosis mptC* homologue is essential for biosynthesis of the second and possibly third man*p* residue of the mannose cap of LAM, lysates of wildtype *M. marinum* and *mptC* mutant were analysed by SDS-PAGE and immunoblot to investigate different LAM structures. We used the monoclonal antibodies F30-5 recognizing the arabinan branches of LAM (α-AraLAM) (Kolk *et al.*, 1984; Appelmelk *et al.*, 2008) and F55.92.1a1, indicative for the presence of the first α(1→5)-linked man*p* residue on LAM (α-ManLAM) (Appelmelk *et al.*, 2008). Additionally, immunoblots were probed with horseradish peroxidase (HRP)-conjugated cyanovirin (CV-N) to detect mycobacterial di- or trimannoside capped LAM ($Man_{2/3}$LAM) (Driessen *et al.*, 2012). As a control strain, we included the previously described *M. marinum* capless mutant which has a transposon inserted in gene *mmar_2439* (*capA*, orthologue of *M. tuberculosis Rv1635c*) encoding the α(1→5) mannosyltransferase responsible for adding the first mannosyl residue of the mannose cap to LAM (Dinadayala *et al.*, 2006; Appelmelk *et al.*, 2008).

All strains reacted well with α-AraLAM, indicating that the basic structure of LAM is unaffected (Fig. 3A). In contrast to the capless mutant, staining with α-ManLAM was observed for the *mptC* mutant, which reflects the presence of a monomannoside cap (Fig. 3B). As expected, immunoblots probed with α-AraLAM and α-ManLAM revealed that *mptC* mutant LAM migrated faster than wildtype LAM, indicating the absence of α(1→2)-linked

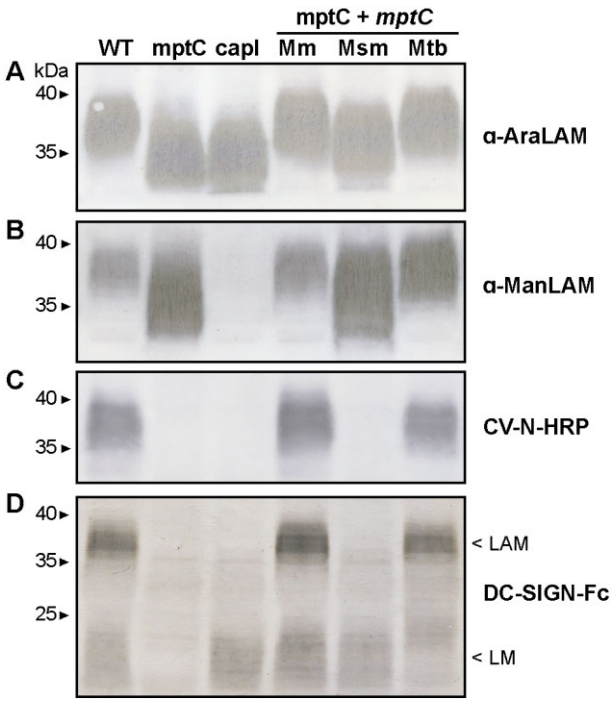


**Fig. 3.** Mannose cap elongation and mannan core branching disrupted in *mptC* mutant. Immunoblots of lysates of wildtype *M. marinum* (WT), the *mptC* mutant (mptC), the capless mutant (capl), the *mptC* mutant complemented with *M. marinum*, *M. smegmatis* or *M. tuberculosis mptC*, (mptC + *mptC* Mm, Msm and Mtb respectively). Samples were separated by SDS-PAGE and probed with (A) Mab F30-5 (α-AraLAM), (B) Mab F55.92.1a1 (α-ManLAM), (C) CV-N-HRP or (D) DC-SIGN-Fc.

mannosyl units. Upon probing with CV-N-HRP, the wildtype showed a clear reaction at the position of LAM, whereas neither the *mptC* nor the capless mutant showed reactivity (Fig. 3C), demonstrating the absence of the second and third mannose capping residue. Immunoblot analysis of the complemented *mptC* mutants expressing either *M. marinum* or *M. tuberculosis mptC* resulted in reactivity similar to that of the wildtype, both with regard to LAM migration pattern as well as for $Man_{2/3}$LAM staining (Fig. 3A–C).

To analyse if, in addition to LAM, also LM of the *mptC* mutant was affected by the mutation, we probed with a DC-SIGN-Fc construct, because both ManLAM and LM are DC-SIGN ligands (Maeda *et al*., 2003; Pitarque *et al*., 2005; Torrelles *et al*., 2006). Immunoblots of wildtype *M. marinum* probed with DC-SIGN-Fc revealed two distinct products, representing LAM and LM, as migration patterns correspond to that of LAM and LM (Fig. 3D). Whereas the capless mutant only lacked the upper signal, the *mptC* mutant showed also no staining at the position of LM. Introduction of either *M. marinum* or *M. tuberculosis mptC* reverted the altered reactivity to DC-SIGN-Fc to wildtype phenotype (Fig. 3D). These data support previous reports on the role of MptC in adding α(1→2)-man*p* side-chains to LM and LAM in *M. tuberculosis* (Kaur *et al*., 2008; Sena *et al*., 2010; Mishra *et al*., 2011b). Collectively, our data indicate that the *M. marinum mptC* mutant is defective in both mannose cap extension of LAM as well as mannan core branching of LM and LAM.

### *Chemical characterization of LM and LAM of the* M. marinum *mptC mutant*

To further demonstrate the involvement of MptC in glycoconjugate biosynthesis, we decided to analyse LAM, LM and PIMs from the strains in detail. In accordance with the immunoblot results, there were substantial differences between wildtype and *mptC* mutant lipoglycan profiles on SDS-PAGE (Fig. 4A). Migration patterns of the crude extracts confirmed that LAM from the *mptC* mutant is smaller in size than wildtype LAM. We observed accumulation of smaller LM in the *M. marinum mptC* mutant (Fig. 4A), indicating that the LM structure is indeed affected by the mutation similar to *M. tuberculosis* and *C. glutamicum* (Kaur *et al*., 2008; Mishra *et al*., 2011b). However, in one of the other studies with *M. smegmatis* deletion of *mptC* resulted in abrogation of LM synthesis (Kaur *et al*., 2006). Absence or/and presence of LM in different species is an indication of a complicated regulation of these macromolecules in different species and further studies are required to explain this phenomenon. Complementation of the *mptC* mutant with either *M. marinum* or *M. tuberculosis mptC* restored the wildtype phenotype (Fig. 4B).

Crude lipoglycan preparations were further purified using ion-exchange and gel filtration chromatography and pure LM and LAM were analysed using nuclear magnetic resonance (NMR). As previously described major resonance of $^{1}$H spectrum corresponding to different glycosyl linkages are found between δ5.50 and δ4.90. Based on previous work from ourselves (Birch *et al*., 2010; Mishra *et al*., 2011b) and others (Nigou *et al*., 1999; Kaur *et al*., 2008), we assigned the $^{13}$C resonance at δ101 ppm that correlated to an anomeric proton at δ5.15 ppm to 2,6-α-man*p* (core) and 2-α-man*p* (cap). The $^{13}$C resonances at δ105 and δ102.3, correlating to protons at δ5.07 and δ4.90, were assigned to *t*-man*p* and 6-man*p* respectively. The *t*-β-ara*f* and 5-β-ara*f* residues corresponded to δ103.4 with $^{1}$H at δ5.16. The well-separated two spin systems for 2-α-ara*f* attached to the 3-position (2-α-ara*f*→3, δ108.2, δ5.27 ppm) and the 5-position (2-α-ara*f*→5, δ108.5, δ5.20) of the 3,5-ara*f* were also observed. Similarly, δ110.3 and δ5.19 ppm, δ110.3 and δ5.14 ppm, and δ110.3 and δ5.11 ppm were assigned to 5-α-ara*f*, 3,5-α-ara*f* and 3,5-α-ara*f* overlapping 5-α-ara*f* in different chemical environments (Nigou *et al*., 1999; Birch

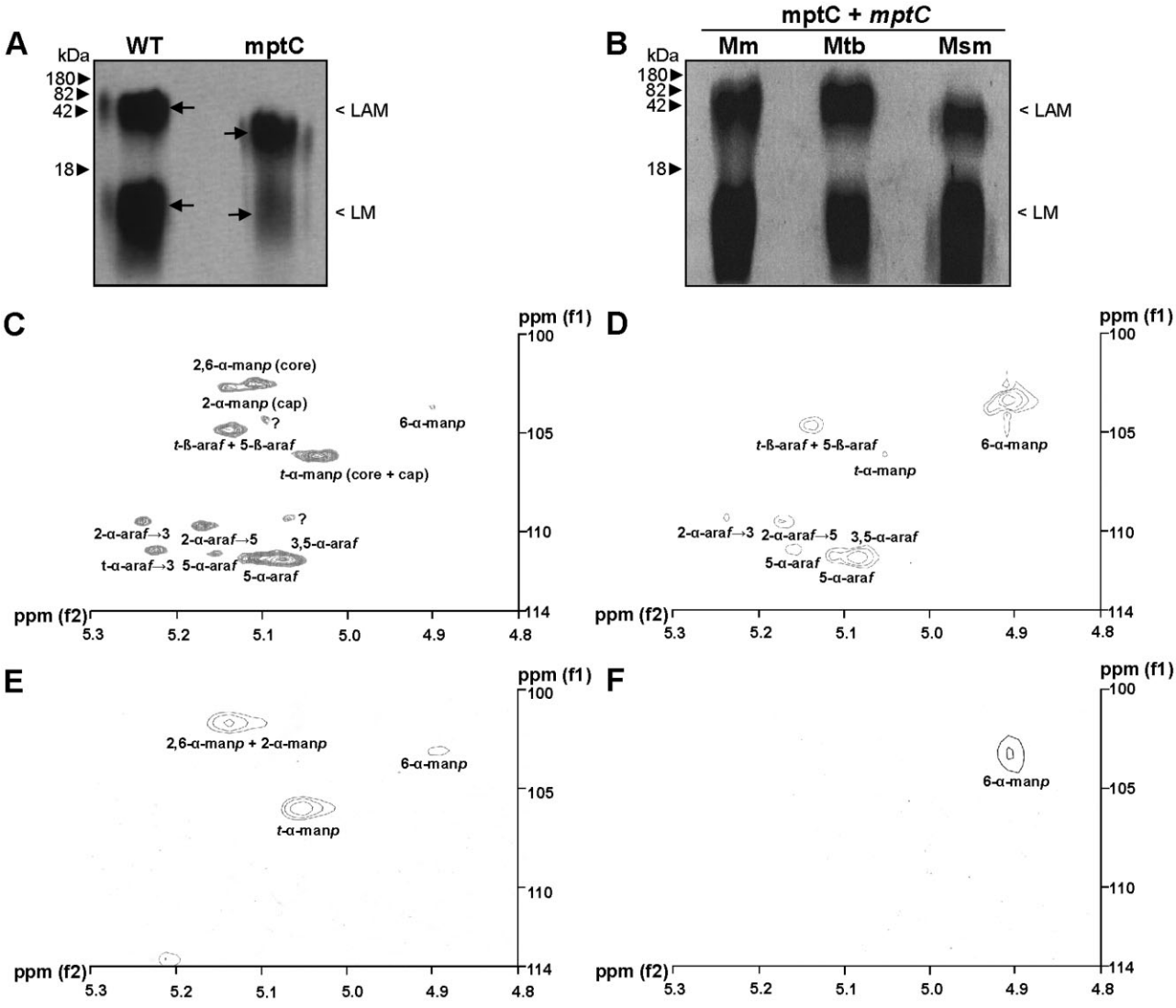


**Fig. 4.** Analysis of lipoglycan profiles confirms disrupted mannan core branching in *mptC* mutant.
A and B. Lipoglycans extracted from (A) wildtype *M. marinum* (WT) and the *mptC* mutant (mptC), or (B) the *mptC* mutant complemented with *M. marinum*, *M. tuberculosis* or *M. smegmatis mptC* (mptC + *mptC* Mm, Mtb and Msm respectively) were run on SDS-PAGE and visualized using Pro-Q emerald glycoprotein stain (Invitrogen). Arrows in A indicate 'Centre of Maxima' (CoM) of these heterogeneous lipoglycan species. C–F. Two dimensional $^{1}$H-$^{13}$C-NMR heteronuclear multiple-quantum correlation (HMQC) spectra from lipoglycans from wildtype *M. marinum* and *mptC* mutant. LAM (C and D) and LM (E and F) were extracted and purified from *M. marinum* and the *mptC* mutant respectively, and their 2D $^{1}$H-$^{13}$C-NMR HMQC spectra were recorded. Various chemical resonances were annotated to their respective linkages based on previous work (Nigou *et al.*, 1999; Kaur *et al.*, 2008).

*et al.*, 2010). In comparison to wildtype *M. marinum* LAM, the *mptC* mutant LAM spectrum was less complex and the resonances associated with the arabinan domain (*t*-β-ara*f*, 5-β-ara*f*, 2-α-ara*f*→3, 2-α-ara*f*→5, 5-α-ara*f*, 3,5-α-ara*f* and 3,5-α-ara*f*) are conserved (Fig. 4C and D). As expected, spin systems at δ101 ppm and δ5.15 ppm corresponding to 2,6-α-man*p* (core) and 2-α-man*p* (cap) were absent in the mutant. Additionally, the spin systems at δ105 and δ5.07 corresponding to *t*-man*p* were also absent, while there was a concomitant increase in δ102.3 and δ4.90 assigned to 6-α-man*p*. Wildtype LM gave strong signals for 2,6-α-man*p* and *t*-man*p*, and weak signal for 6-α-man*p*. As expected, spin systems for 2,6-α-man*p* and *t*-man*p* were almost absent with a concomitant increase in 6-α-man*p* in *mptC* mutant LM (Fig. 4E and F). In summary, this analysis suggests that as compared with wildtype LAM, *mptC* mutant LAM has an unaltered arabinan domain composed of 5-α-ara*f* branched with 3,5-α-ara*f*, which is further extended with 5-α-ara*f* leading to tetra and hexa arabinan motifs and terminated

**Table 1.** Linkage analysis of lipoglycans.

| lipoglycan sample | *t*-α-man*p* (%) | *2,6*-α-man*p* (%) | *6*-α-man*p* (%) |
|---|---|---|---|
| *M. marinum* wildtype LAM | 40 | 37 | 23 |
| *mptC* mutant LAM | 7 | 0 | 93 |
| *mptC* mutant + Mm-*mptC* LAM | 41 | 37 | 22 |
| *mptC* mutant + Mtb-*mptC* LAM | 38 | 35 | 27 |
| *mptC* mutant + Msm-*mptC* LAM | 37 | 34 | 29 |
| *M. marinum* wildtype LM | 42 | 38 | 20 |
| *mptC* mutant LM | 8 | 0 | 92 |
| *mptC* mutant + Mm-*mptC* LM | 43 | 38 | 19 |
| *mptC* mutant + Mtb-*mptC* LM | 40 | 36 | 24 |
| *mptC* mutant + Msm-*mptC* LM | 39 | 36 | 25 |

Molar ratios of various mannan linkages were determined from peak integration of GC-MS peaks. Various linkages were calculated considering total mannan content in each lipoglycan species as 100% (Kaur *et al*., 2008; Birch *et al*., 2010). Because disruption of *mptC* had no effect on arabinan linkages, only mannan core linkages are shown here.

with *t*-β-ara*f*. The mannan core of *mptC* mutant LAM and LM is composed of linear 6-α-man*p* units without *t*-man*p*.

Gas chromatography mass spectrometry (GC-MS) of per-*O*-methylated alditol acetate derivatives confirmed these findings and showed an unaltered glycosidic linkage profile for the arabinan domain of both wildtype *M. marinum* and *mptC* mutant LAM and a complete loss of branching mannan units from *mptC* mutant LAM and LM (Table 1). Complementation of the *mptC* mutant with either *M. marinum* or *M. tuberculosis mptC* restored the glycosyl linkage profile to that of wildtype (Table 1), confirming that *mmar_3225* and *Rv2181* are functional orthologues. Additionally, to confirm that the transposon insertion led to a complete inactivation of α(1→2) mannosyltransferase activity, we performed an α(1→2) mannosyltransferase assay with membrane fractions of the different strains and synthetic nonasaccharide acceptor, azidoethyl 6-*O*-benzyl-α-D-mannopyranosyl-(1→6)-[α-D-mannopyranosyl-(1→6)]$_7$-D-mannopyranoside (Acc-Man$_9$) and the donor polyprenyl-phosphomannose (PP-[$^{14}$C]-M) as described before (Mishra *et al*., 2011b). These results showed that the disruption of *mptC* in *M. marinum* resulted in a complete abrogation of α(1→2) mannosyltransferase activity (Fig. S2). Complementation with either *M. marinum* or *M. tuberculosis mptC* restored this activity to wildtype levels. Finally, we analysed PIM profiles on two-dimensional thin layer chromatography (2D-TLC) and matrix assisted laser desorption/ionization mass spectrometry (MALDI-TOF-MS) and did not observe any change in the *mptC* mutant as compared with wildtype *M. marinum* (Fig. S3 and data not shown). Collectively, our data demonstrate that both α(1→2) mannan core branching of LM and LAM and α(1→2) mannose cap extension of LAM are defective in our *M. marinum mptC* mutant.

### *Role of discrete structural LM or LAM motifs in virulence*

Because the α(1→2) mannosyltransferase has a dual role in LM and LAM biosynthesis, we attempted to define which structural motifs of the molecules are involved in virulence.

First, we analysed whether the absence of LAM capping was responsible for the attenuated phenotype by testing the *M. marinum* capless mutant. Previously it was shown that the capless mutant persisted equally well as wildtype *M. marinum* in macrophages and adult zebrafish (Appelmelk *et al*., 2008). We examined if this was also the case in our zebrafish embryo assay. In accordance with the earlier reported phenotype *in vitro* and in adult fish, no attenuation of the capless mutant was observed in embryos (Fig. 1B and C). These results confirm that the mannose caps on LAM are not essential for virulence. We hypothesized that either the presence of a mono-mannoside cap on LAM or the absence of mannose branching of the mannan core of LM and/or LAM accounts for the attenuation of our *mptC* mutant.

To investigate the possibility that the attenuation was a result of the lack of mannan backbone branching, we complemented the *mptC* mutant with the *M. smegmatis mptC* orthologue *MSMEG_4247*. Expression of this *M. smegmatis* orthologue in the *mptC* mutant enabled us to differentiate the two roles of *M. marinum* MptC. Like its *M. tuberculosis* orthologue, the mannosyltransferase encoded by *MSMEG_4247* is involved in addition of mannose branches to the LAM and LM mannan core. However, it has no function in capping of LAM (Kaur *et al*., 2006; Sena *et al*., 2010). Indeed, the glycosidic linkage analysis of the *mptC* mutant complemented with the *M. smegmatis mptC* demonstrated that mannose branches were present on LAM (Table 1). These data were supported by the α-ManLAM and α-AraLAM immunoblots and migration patterns of crude extracts, as the overall apparent molecular weight of LAM was slightly increased as compared with that of *mptC* mutant LAM (Figs 3A, B and 4B). In accordance with its predicted function, introduction of *M. smegmatis mptC* did not restore LAM capping of the *mptC* mutant as shown with immunoblots probed with CV-N-HRP and DC-SIGN-Fc (Fig. 3C and D). The DC-SIGN-Fc immunoblot, the migration pattern of purified LM on SDS-PAGE, and the glycosidic linkage profile also indicated that the biosynthesis of LM in the complemented strain was comparable to that of wildtype (Figs 3D, 4B and Table 1). We then analysed the *in vivo* phenotype of the *mptC* mutant complemented with *M. smegmatis mptC* in embryos.

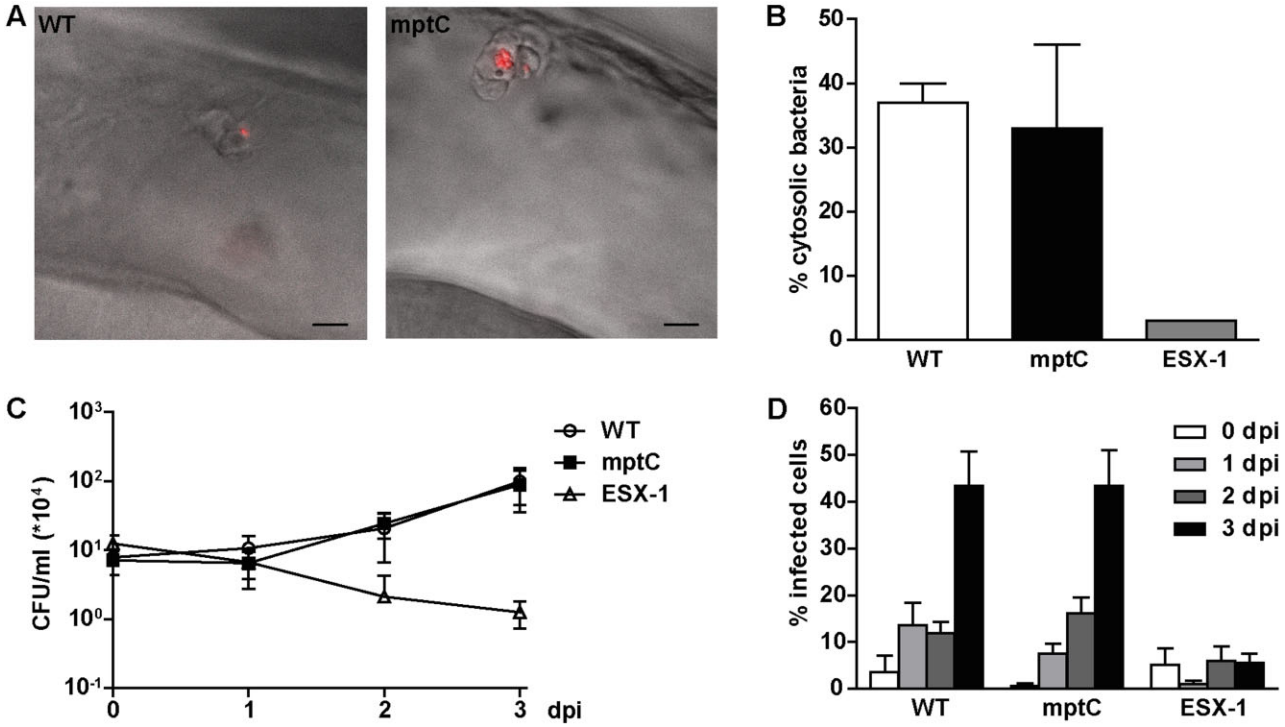


**Fig. 5.** Initial survival of *mptC* mutant in macrophages not affected.
A. Overlay of differential interference contrast and fluorescent images of lateral view of the hindbrain ventricle of embryos at 4 h post infection with wildtype *M. marinum* (WT) or the *mptC* mutant (mptC). Highly activated macrophages on the roof of the ventricle have engulfed the bacteria. Scale bars represent 10 μm.
B. Translocation of wildtype *M. marinum*, the *mptC* mutant and the ESX-1 deficient *eccCb1*::tn mutant (ESX-1) in THP-1 macrophage-like cells. Cells were infected for 24 h at MOI 10 and the percentage of cytosolic bacteria was determined by electron microscope analysis. Data shown for wildtype and *mptC* mutant represent mean + SEM of two independent experiments, 465 individual bacteria in infected THP-1 were counted. For the *eccCb1*::tn mutant one sample was analysed.
C. Intracellular growth of wildtype *M. marinum*, the *mptC* mutant and the *eccCb1*::tn mutant in THP-1 cells. Infections were performed at MOI 0.5 and colony forming units were determined by lysing infected cells and plating lysates at indicated timepoints. The graph represents mean ± SEM of three independent replicates.
D. Intercellular spread of wildtype *M. marinum*, the *mptC* mutant and the *eccCb1*::tn mutant. THP-1 cells were infected at MOI 0.5 and the percentage of infected cells was determined by microscopic enumeration of infected cells. Three representative microscopic fields with each ~ 50–250 THP-1 cells were counted per experiment. Mean + SEM of three independent experiments is shown.

These results showed that expression of *M. smegmatis mptC* restored the attenuation of the *mptC* mutant to wildtype levels (Fig. 1A–C). In conclusion, our data are consistent with the hypothesis that the attenuation of virulence of the *mptC* mutant is not a result of defective cap elongation but a direct consequence of defective α(1→2) mannosyl branching of the mannan core of LAM and/or LM.

### *Analysis of the phenotype of the* M. marinum *mptC mutant in macrophages*

Next, we attempted to unravel the basis of attenuation of the *mptC* mutant. The first step in mycobacterial pathogenicity is the internalization of mycobacteria into their primary host cell, the macrophage. Recruitment of macrophages to the site of infection, as well as phagocytosis of bacteria can be assessed *in vivo* by injecting bacteria in the hind brain ventricle of embryos at 1 dpf (Herbomel *et al*., 2001; Davis *et al*., 2002). The hind brain ventricle is a closed cavity, where macrophages are usually absent (Herbomel *et al*., 2001). Ventricle infection experiments indicated that recruitment of macrophages to the site of infection and phagocytosis of bacteria do not depend on MptC, as shortly after infection with both wildtype and *mptC* mutant multiple macrophages were recruited to the ventricle and internalization of bacteria was observed (Fig. 5A).

Next, we explored the capacity of the *mptC* mutant to persist inside macrophages *in vitro*. A strategy used by mycobacteria to circumvent eradication in phagolysosomes is translocation from the phago(lyso)some into the cytosol, where bacterial replication takes place (Stamm *et al*., 2003; van der Wel *et al*., 2007). To analyse if this step is affected in the *mptC* mutant, we infected macrophages with wildtype *M. marinum* and the *mptC*

mutant and analysed subcellular localization of bacteria by electron microscopy. As a control, we included the ESX-1 deficient *eccCb1*::tn mutant, because a functional ESX-1 secretion system is required for translocation (van der Wel *et al*., 2007; Houben *et al*., 2012). The percentage of cytosolic *mptC* mutant bacteria was comparable to that of the wildtype, whereas translocation of the *eccCb1*::tn mutant was strongly affected (Fig. 5B and Fig. S4).

Previous research showed that mannose-capped LAM is required for blocking phagosomal maturation and subsequent survival of mycobacteria in macrophages (Fratti *et al*., 2003; Vergne *et al*., 2003; Hmama *et al*., 2004; Kang *et al*., 2005). Therefore, we infected macrophages with wildtype *M. marinum* and the *mptC* mutant and determined intracellular replication and intercellular spread. Again, the *eccCb1*::tn mutant served as a control, because this strain is known to be attenuated for growth and spread in macrophages (Stoop *et al*., 2011). Strikingly, the *mptC* mutant replicated and spread equally well as the wildtype strain, while the *eccCb1*::tn mutant was strongly attenuated in both assays (Fig. 5C and D). Similar cfu counts for wildtype and *mptC* mutant at time 0 of infection implied that both strains are being internalized to the same extent, which corroborates our *in vivo* hind brain infection results. These experiments suggest that the attenuated phenotype of the *mptC* mutant observed *in vivo* is not due to defective entry or initial persistence in macrophages.

### *Phenotype of the mptC mutant in adult zebrafish*

The zebrafish embryo model enables us to study virulence and early granuloma formation solely in the context of innate immunity. However, the development of mature granulomas also depends on adaptive immunity. To evaluate whether the *mptC* mutant is also attenuated when infection is initiated in the presence of an adaptive immune system, we performed adult zebrafish infections. Fish were infected intraperitoneally with wildtype bacteria or the *mptC* mutant. Granuloma formation was assessed by HE staining and bacterial replication was monitored by determining colony forming units in spleens and livers.

Infection with the *mptC* mutant resulted in systemic disease with granulomas in multiple organs. Although at 4 weeks post infection (wpi) the total number of granulomas in *mptC* mutant infected fish was significantly lower in comparison to wildtype infected fish (Fig. 6A), bacterial growth of the *mptC* mutant was only moderately reduced. In spleens of fish infected with the *mptC* mutant the mean bacterial load was 10-fold lower than the load of wildtype *M. marinum* infected spleens, but no differences in bacterial growth in livers were observed (Fig. 6B). At 8 wpi, when mature granulomas had formed, comparable numbers of granulomas were found in wildtype and *mptC* mutant infected fish (Fig. 6C). The percentage of mature granulomas, characterized by central necrosis, that are typical for progressive disease (Swaim *et al*., 2006) in fish infected with mutant bacteria was similar to that in wildtype infected animals (44 versus 59% respectively; $P > 0.05$). However, both early and late in infection, we observed differences in the granuloma morphology in fish infected with wildtype or *mptC* mutant. In *mptC* mutant infected zebrafish, granulomas were generally more compact and less tissue destruction was observed in comparison to wildtype infected fish (Fig. 6D). Altogether, these data demonstrate that attenuation of the *mptC* mutant is less prominent in the context of an adaptive immune system.

## Discussion

Current knowledge on the role of LM and LAM in mycobacterial virulence has mainly resulted from *in vitro* studies with purified material (Nigou *et al*., 2001; Hmama *et al*., 2004; Torrelles *et al*., 2011; Wu *et al*., 2011). Although it has been assumed that mannose caps of LAM are important structural features of virulent mycobacteria to subvert the immunological defence of the host, *in vivo* data indicated that mannose capping does not affect virulence (Appelmelk *et al*., 2008; Festjens *et al*., 2011; Afonso-Barroso *et al*., 2012). Strikingly, Fukuda *et al*. recently showed that a *M. tuberculosis mptC* mutant was not attenuated for virulence in adult mice, although structural alterations in LM and LAM due to overexpression of *mptC* did affect bacterial growth and virulence *in vivo* (Fukuda *et al*., 2013). Our screen for mycobacterial factors involved in granuloma formation led to the identification of a *M. marinum* mutant with an altered LM and LAM mannosylation pattern that is strongly attenuated for virulence in the zebrafish embryo model of infection. We demonstrate that in this mutant, disruption of the *mptC* gene results in the absence of $\alpha(1\rightarrow2)$-linked di- and trimannoside caps of LAM as well as in loss of $\alpha(1\rightarrow2)$-linked mannose branching residues on the mannan core of LM and LAM (Fig. S1). The phenotype of the *M. marinum mptC* mutant in terms of chemical structure of LM/LAM is similar to that of a *M. tuberculosis mptC* mutant (Kaur *et al*., 2008; Sena *et al*., 2010), and by complementation of the *M. marinum* mutant with the *M. tuberculosis mptC* orthologue we could demonstrate that the two genes are functionally conserved.

The unique property of the zebrafish model to study the first stages of granuloma formation solely in the context of innate immunity allowed us to identify a role for LM and/or LAM in mycobacterial virulence. Upon initiation of infection in the context of an adaptive immune system,

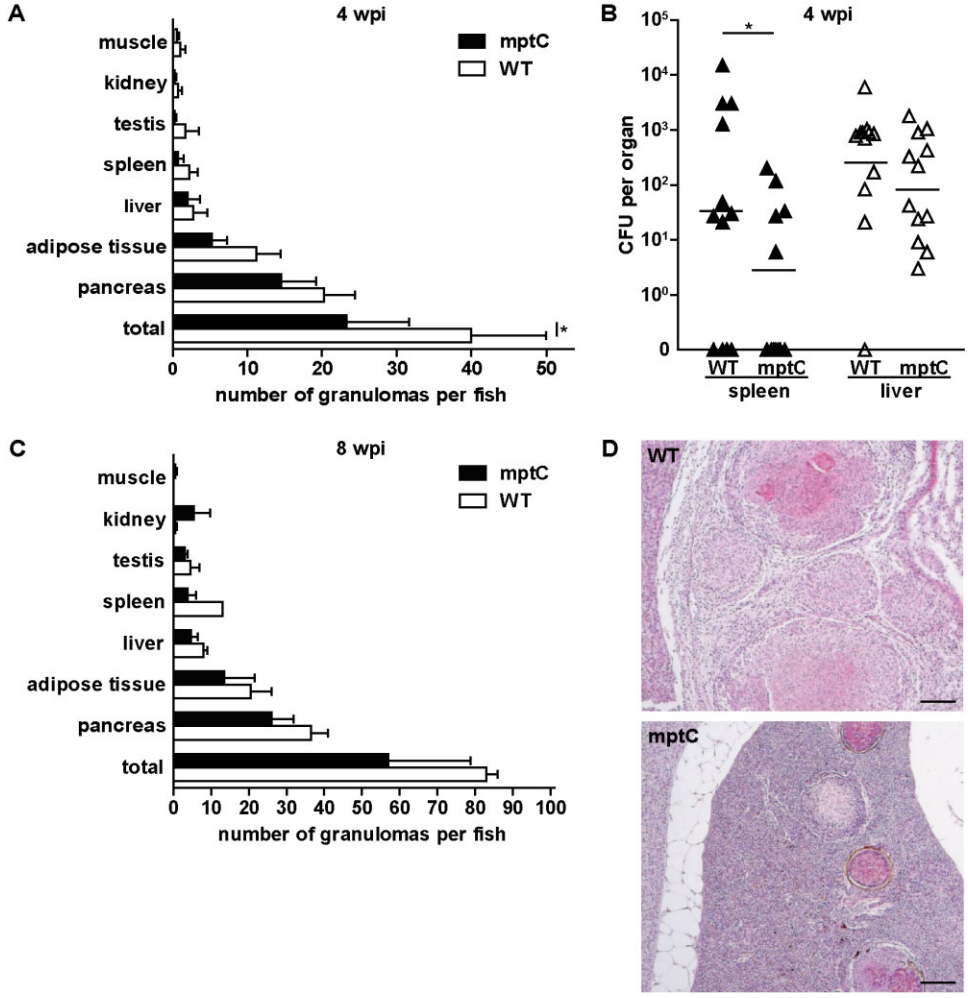


**Fig. 6.** MptC has a minor effect on virulence in adult zebrafish. Adult fish intraperitoneally infected with $4 \times 10^3$ cfu wildtype *M. marinum* (WT) or $6 \times 10^3$ cfu *mptC* mutant (mptC).

A. Amount of granulomas per fish and tissue distribution at 4 wpi with wildtype *M. marinum* and *mptC* mutant. Four animals per group were terminated and processed for histological analysis. The graph represents mean + SEM. $^*P < 0.05$, two-way ANOVA, Bonferroni's multiple comparison test.

B. Bacterial load of infected fish spleens and livers at 4 wpi. Twelve fish per bacterial strain were analysed and bars indicate mean after log transformation. ND, not detected. $^*P < 0.05$, two-way ANOVA, Bonferroni's multiple comparison test on log transformed data.

C. Amount of granulomas per fish and tissue distribution at 8 wpi. Two wildtype infected fish and four *mptC* mutant infected fish were analysed. The graph represents mean + SEM.

D. Histopathology of fish at 8 wpi with wildtype *M. marinum* or *mptC* mutant. Representative haematoxylin and eosin (HE) staining of splenic lesions observed at low magnification. Bars represent 100 μm.

differences between *mptC* mutant and wildtype *M. marinum* were less apparent. Interestingly, the adult infection data are in accordance with those found in a study with a *M. bovis* BCG *mptC* mutant, which showed small but significant differences in initial bacterial growth and granuloma formation in a mice model of infection (Festjens *et al.*, 2011).

In order to elucidate the structural entity responsible for the attenuation of the *mptC* mutant, we introduced the *M. smegmatis mptC* (Kaur *et al.*, 2006) in the mutant, which restored mannan core branching whereas elongation of monomannoside caps was still defective (Fig. S1). Strikingly, restoration of mannan core branching in the *mptC* mutant was sufficient to fully complement the *in vivo* phenotype in embryos. This demonstrates that not LAM capping but mannan core branching of LM and/or LAM is a virulence determining factor in the context of innate immunity.

As an alternative explanation for the attenuated phenotype of the *mptC* mutant, we hypothesized that the presence of monomannoside-capped LAM is detrimental for virulence in zebrafish embryos. Because the presence of ManLAM in the mycobacterial cell wall has only been described for slow-growing, pathogenic mycobacteria

(Nigou *et al*., 1997; Khoo *et al*., 2001; Guerardel *et al*., 2003), it has been assumed that mannose caps on LAM co-evolved with virulence. However, a recent study revealed that in some rapid-growing non-pathogenic mycobacterial species monomannoside caps are present on LAM (N.N. Driessen *et al*., in preparation). In that study, elongation of the cap and the presence of di- and trimannoside caps on LAM was indeed found to be restricted to the slow-growing species. These results may suggest that monomannoside-capped LAM is disadvantageous for mycobacterial virulence. However, because the *in vivo* phenotype of the *mptC* mutant complemented with the *M. smegmatis mptC* did not differ considerably from the phenotype of wildtype *M. marinum* or the capless mutant, we conclude that monomannoside capped LAM does not decrease infection capacity as compared with fully capped or uncapped LAM. This conclusion is supported by the fact that the main capping motif of *M. marinum* is monomannoside (Pitarque *et al*., 2005). Yet, the data do not allow us to exclude that the attenuation of the *mptC* mutant is the result of a synergistic effect of defective mannan core branching and cap elongation of LAM. It is possible that with the shortened monomannoside capped arabinan domain, the mannan core becomes more accessible to pattern recognition receptors, as was previously shown for LAM of a *M. smegmatis aftC* deletion mutant with a truncated arabinan domain (Birch *et al*., 2010) or LAM of *M. kansasii* with an enzymatically truncated arabinan moiety (Vignal *et al*., 2003). However, this possibility does not seem likely, because differences in arabinan domain length will be negligible.

The best studied effect of purified ManLAM is its capacity to induce phagosomal maturation arrest (Fratti *et al*., 2003; Vergne *et al*., 2003; Hmama *et al*., 2004; Kang *et al*., 2005). We analysed entry, subcellular localization, replication and spread of the *mptC* mutant in macrophages. Surprisingly, all macrophage experiments showed that the *mptC* mutant did not differ from the wildtype strain. Because a reduced ability to arrest phagosomal maturation would probably affect intracellular survival, we conclude that phagosomal maturation arrest of the *mptC* mutant is not significantly affected. Our data are in agreement with a study demonstrating that the *M. bovis* BCG *mptC* mutant did not differ from wildtype *M. bovis* BCG *in vitro* (Festjens *et al*., 2011).

In addition to effects on phagosomal maturation, ManLAM has been shown to bind DC-SIGN, thereby suppressing DC maturation and skewing cell mediated immunity to interfere with induction of a protective anti-TB immune response (Geijtenbeek *et al*., 2003; Maeda *et al*., 2003; Tailleux *et al*., 2003; Wu *et al*., 2011). We show that binding of a DC-SIGN-Fc construct to both LAM and LM in lysates of the *mptC* mutant was affected. This confirms that the DC-SIGN-LAM binding depends on mannose capping residues and indicates that mannose branches on LM are important for DC-SIGN-LM interaction. However, it remains to be determined whether binding of intact bacteria to DC-SIGN is impaired, as for unknown reasons, binding of intact *M. marinum* bacteria to DC-SIGN expressed on human DCs cannot be detected (Pitarque *et al*., 2005; Appelmelk *et al*., 2008). Moreover, because attenuation of the *mptC* mutant is primarily observed in the context of innate immunity, and zebrafish DCs are not detected before 5–7 dpf (Lugo-Villarino *et al*., 2010; Wittamer *et al*., 2011), it is unlikely that the observed phenotype results from a disrupted DC-SIGN binding and/or DC modulation.

It seems reasonable to assign the mutant phenotype to defective mannan core $\alpha(1\rightarrow2)$ branching. Multiple studies have emphasized the potency of the mannan core of both LM and (truncated) LAM to induce innate TLR-2 responses (Vignal *et al*., 2003; Dao *et al*., 2004; Quesniaux *et al*., 2004; Doz *et al*., 2007; Nigou *et al*., 2008; Birch *et al*., 2010). The level of mannan core branching is one of the structural features that determines TLR-2 activity (Nigou *et al*., 2008). Further studies are required to determine if attenuation of the *mptC* mutant can be attributed to enhanced TLR-2 signalling. Unfortunately, as a single mannosyltransferase is responsible for both branching of the mannan core and elongation of the mannose cap, it is not possible to separate these functions and study the effect of a mutant exclusively disrupted in mannan core branching. It is also impossible to identify whether mutated LM or LAM is the major contributor to the observed *in vivo* phenotype.

Despite the role of LM/LAM during early granuloma formation, our data do not strengthen the idea of utilization of such a mutant strain for the development of novel vaccines, especially if this mutation is not combined with other mutations. It is intriguing though that in the *M. marinum* zebrafish infection model an effect of LM and/or LAM mannan core branching on virulence can be shown. Our study demonstrates for the first time that mannan core branching of LM and/or LAM is important for virulence in the context of innate immunity and confirms that the immunological properties assigned to purified mannose capped LAM are irrelevant *in vivo*.

## Experimental procedures

### *Bacteria and growth conditions*

*Mycobacterium marinum* strain E11 and the *Escherichia coli* strain DH5$\alpha$ were cultured as previously described (Stoop *et al*., 2011).

### *Identification of genes involved in early granuloma formation in zebrafish embryos*

A transposon mutant library was generated in *M. marinum* strain E11 (Mma11) containing pSMT3-mcherry and 1000 individual mutants were screened for their ability to initiate granuloma formation in embryonic zebrafish (*Danio rerio*) using our previously described method (Stoop *et al*., 2011). Briefly, embryos were infected at ~ 28 h post fertilization with 50–200 colony forming units of bacterial suspension injected into the caudal vein. At 5 dpi infected embryos were monitored with fluorescence microscopy. Bacterial mutants that repeatedly showed significantly reduced early granuloma formation as compared with the wildtype *M. marinum*, as determined by custom-designed software, were selected. Transposon insertion sites were determined by ligation-mediated PCR and sequence analysis. All procedures involving zebrafish embryos were performed in compliance with local animal welfare laws.

### *Determination of bacterial loads of infected embryos*

Embryo lysates were prepared as described previously (Stoop *et al*., 2011). Shortly, embryos were dissociated in the presence of 5% (w/v) SDS, lysed and decontaminated by incubation with MycoPrep reagent (BD Bioscience), neutralized with phosphate buffered saline (PBS) and serial dilutions were plated.

### *Immunoblotting assay*

Bacteria grown to exponential phase were lysed by bead-beating (Biospec). Samples were normalized to total protein concentration using BCA Protein Assay (Pierce), separated by SDS-PAGE, transferred to a PVDF membrane (Millipore) and immunostained as previously described (Appelmelk *et al*., 2008; Driessen *et al*., 2010; 2012).

### *Chemical analysis of LM and LAM*

Polar and apolar lipids were extracted and examined by two dimensional thin-layer chromatography (2D-TLC) on aluminum backed plates of silica gel 60 $F_{254}$ (Merck 5554), using $CHCl_3$/$CH_3OH$/$H_2O$ (65:25:4, v/v/v) in the first direction and $CHCl_3$/$CH_3COOH$/$CH_3OH$/$H_2O$ (40:25:3:6, v/v/v/v) in the second direction as previously described (Dobson *et al*., 1995). Glycolipids were visualized by spraying plates with α-naphthol/sulfuric acid, followed by gentle charring of the plates. Lipoglycans were extracted from delipidated cells as previously described (Nigou *et al*., 1997; Ludwiczak *et al*., 2001; 2002) and crude lipoglycan extracts were further subjected to Octyl Sepharose CL-4B and Sephacryl S-200 (2.5 cm × 50 cm) gel filtration chromatography to separate LM and LAM in different fractions (Mishra *et al*., 2011b). For determining the sugar linkages, lipoglycans were per-*O*-methylated, hydrolysed, reduced and per-*O*-acetylated. The resulting alditol acetates were analysed and identified using GC-MS as described previously (Tatituri *et al*., 2007). NMR spectra were recorded on a Bruker DMX-500 equipped with a double resonance (1H/X)-BBi z-gradient probe head. All samples were exchanged in $D_2O$ (D, 99.97% from Euriso-top, Saint-Aubin, France), with intermediate lyophilization, and then dissolved in 0.5 ml $D_2O$ and analysed at 313 K. The $^1H$ and $^{13}C$ NMR chemical shifts were referenced relative to internal acetone at 2.225 and 34.00 ppm respectively. All the details concerning NMR sequences used and experimental procedures were described in previous studies (Gilleron *et al*., 2000).

### In vitro *α(1→2)-mannopyranosyltransferase assay*

α(1→2)-Mannosyltransferase activity was determined using synthetic nonasaccharide acceptor, azidoethyl 6-*O*-benzyl-α-D-mannopyranosyl-(1→6)-[α-D-mannopyranosyl-(1→6)]$_7$-D-mannopyranoside (Acc-$Man_9$) and the donor polyprenyl-phosphomannose (PP-[$^{14}$C]-M) in a cell-free assay using 1 mg of membrane protein as described previously (Mishra *et al*., 2011b). The products of the assay were resuspended in water before scintillation counting. The incorporation of [$^{14}$C]-Man*p* was determined by subtracting counts present in control assays. Blank = synthetic nonasaccharide acceptor, Acc-$Man_9$ and the donor polyprenyl-phosphomannose (PP-[$^{14}$C]-M without any membrane.

### *Complementation of the mptC mutant*

The wildtype *mmar_3225* gene was PCR amplified with *M. marinum* Mma11 genomic DNA as a template using primers mmar_3225-F: aGATATCaggtgcgggtcacaaaaa and mmar_3225-R: aGATATCatcaagaacggcggcaag (uppercase, engineered EcoRV sites). The PCR product was digested with EcoRV and ligated into the StuI site of the integrative and chloramphenicol resistant vector pUC-INT-CAT (Abdallah *et al*., 2009). The *M. tuberculosis* and *M. smegmatis* orthologues *Rv2181* and *MSMEG_4247* were amplified from the *M. tuberculosis* H37Rv or *M. smegmatis* mc$^2$155 genome, respectively, using primers Rv2181-F: TTTAAAgacggtggataaaccgtacaa and Rv2181-R: TTTAAAggtgcaaatcccaattcaac or *MSMEG4247*-F: GATATCat cacgacgtggtggatgt and *MSMEG4247*-R: TTTAAAacgtgaagaag gcaggtgac (uppercase, DraI and EcoRV sites). PCR products were ligated into the pJET1.2 cloning vector (Fermentas), excised with DraI alone or in combination with EcoRV, and the resulting blunt-ended inserts were ligated into pUC-INT-CAT digested with StuI. Resulting plasmids were introduced into the *mptC* mutant by electroporation as described previously (Stoop *et al*., 2011).

### *Hind brain ventricle infection*

Wildtype zebrafish embryos and bacteria were treated as described for caudal vein infection (Stoop *et al*., 2011). At ~ 28 h post fertilization embryos were removed from their chorion and infected by microinjection in the hind brain ventricle. At 4 h post infection embryos were monitored by a ZEISS Axiovert 200 Marianas™ digital imaging microscope as described previously (van der Sar *et al*., 2003).

### *Infection of THP-1 cells and electron microscopy*

Infection of THP-1 monocytic cells was executed as previously described (Stoop *et al*., 2011). Briefly, for analysis of intracellular growth and intercellular spread, THP-1 cells were differentiated

into macrophage-like cells with phorbol myristate acetate (Sigma) and seeded at a density of $3 \times 10^5$ cells $ml^{-1}$ in 24-well plates in the absence or presence of glass coverslips respectively. Bacterial suspensions were passed through a 5 μm filter to remove clumps, added to the cells at a multiplicity of infection (MOI) of 0.5 and incubated for 2 h at 30°C and 5% $CO_2$. Extracellular bacteria were removed by washing with RPMI medium and cells were incubated with fresh medium for the indicated time points at 30°C. For determination of intracellular growth, cells were lysed with 1% Triton X-100 and serial dilutions were plated. To analyse intercellular spread, infected cells on coverslips were fixed with paraformaldehyde and examined microscopically. Samples for electron microscopy were prepared as described previously (van der Wel *et al*., 2007). Differentiated THP-1 cells were infected at a MOI of 10 in 75 $cm^2$ cell culture flasks (Corning), extracellular bacteria were removed by washing infected cells with medium and at 24 h post infection cells were fixed for 2 h with paraformaldehyde and glutaradehyde in PHEM buffer. Cell sections of 60 nm thick, prepared at −120°C, were immunogold-labelled with protein A conjugated to 10 nm gold and primary antibody against LAMP-1 (clone H4A3 from BD Biosciences) or CD63 (M1544 from Sanquin). Sections were examined with a FEI CM10 transmission electron microscope and translocation was quantified in a double blinded fashion.

### *Adult zebrafish experiment*

Adult zebrafish infections were performed following procedures described previously (van der Sar *et al*., 2004) and approved by the local Animal Welfare Committee, under protocol number MM01-02 and MM10-01. Bacteria were declumped with 0.3% Tween-80 in PBS and resuspended in PBS. Wildtype male zebrafish of ~ 1 year old were anaesthetized in 0.02% (w/v) ethyl-3-aminobenzoate methanesulfonate salt (Sigma) and injected intraperitoneally with 10 μl of bacterial suspension. Control fish were injected with the same volume of PBS. Fish were sacrificed by incubation in a high concentration (0.05%) of the anaesthetic. Bacterial counts in livers and spleens of 12 fish per group were evaluated by plating serial dilutions of homogenized organ samples decontaminated with MycoPrep reagent (BD Bioscience) onto 7H10 agar plates. For histopathological examination, fish were terminated and preserved in Dietrich's fixative (30% ethanol, 10% formalin, 2% glacial acetic acid in deionized water) for > 48 h before embedding in paraffin and sectioning. Frontal sections (4–7 μm) were stained with haematoxylin and eosin and observed for signs of infection and granuloma formation with a Zeiss Axioskop light microscope. Images were generated with a Leica DC500 camera.

## Acknowledgements

This work was supported by the Smart Mix Program of the Netherlands Ministry of Economic Affairs and the Netherlands Ministry of Education, Culture and Science. GSB acknowledges support in the form of a Personal Research Chair from Mr James Bardrick, Royal Society Wolfson Research Merit Award, as a former Lister Institute-Jenner Research Fellow, the Medical Research Council and the Wellcome Trust (081569/Z/06/Z). JG is financially supported by the Netherlands Organization for Scientific Research (NOW) through a VENI research grant (016.101.001). We thank Sylvia Bogaards, Eveline Weerdenburg, Nina Hertoghs, Robert van de Weerd for technical support, Wim Schouten for his expert technical assistance and Birgit Witte for help with statistical analyses.

## Conflict of interest

The authors declare no conflicts of interest of any kind.

## References

Abdallah, A.M., Verboom, T., Weerdenburg, E.M., Gey van Pittius, N.C., Mahasha, P.W., Jimenez, C., *et al*. (2009) PPE and PE_PGRS proteins of *Mycobacterium marinum* are transported via the type VII secretion system ESX-5. *Mol Microbiol* **73:** 329–340.

Afonso-Barroso, A., Clark, S.O., Williams, A., Rosa, G.T., Nobrega, C., Silva-Gomes, S., *et al*. (2012) Lipoarabinomannan mannose caps do not affect mycobacterial virulence or the induction of protective immunity in experimental animal models of infection and have minimal impact on in vitro inflammatory responses. *Cell Microbiol* **15:** 660–674.

Alderwick, L.J., Lloyd, G.S., Ghadbane, H., May, J.W., Bhatt, A., Eggeling, L., *et al*. (2011) The C-terminal domain of the Arabinosyltransferase *Mycobacterium tuberculosis* EmbC is a lectin-like carbohydrate binding module. *PLoS Pathog* **7:** e1001299.

Appelmelk, B.J., den Dunnen, J., Driessen, N.N., Ummels, R., Pak, M., Nigou, J., *et al*. (2008) The mannose cap of mycobacterial lipoarabinomannan does not dominate the Mycobacterium-host interaction. *Cell Microbiol* **10:** 930–944.

Besra, G.S., Morehouse, C.B., Rittner, C.M., Waechter, C.J., and Brennan, P.J. (1997) Biosynthesis of mycobacterial lipoarabinomannan. *J Biol Chem* **272:** 18460–18466.

Birch, H.L., Alderwick, L.J., Appelmelk, B.J., Maaskant, J., Bhatt, A., Singh, A., *et al*. (2010) A truncated lipoglycan from mycobacteria with altered immunological properties. *Proc Natl Acad Sci USA* **107:** 2634–2639.

Briken, V., Porcelli, S.A., Besra, G.S., and Kremer, L. (2004) Mycobacterial lipoarabinomannan and related lipoglycans: from biogenesis to modulation of the immune response. *Mol Microbiol* **53:** 391–403.

Broussard, G.W., and Ennis, D.G. (2007) *Mycobacterium marinum* produces long-term chronic infections in medaka: a new animal model for studying human tuberculosis. *Comp Biochem Physiol C Toxicol Pharmacol* **145:** 45–54.

Chan, J., Fan, X.D., Hunter, S.W., Brennan, P.J., and Bloom, B.R. (1991) Lipoarabinomannan, a possible virulence factor involved in persistence of *Mycobacterium tuberculosis* within macrophages. *Infect Immun* **59:** 1755–1761.

Chatterjee, D., Khoo, K.H., McNeil, M.R., Dell, A., Morris, H.R., and Brennan, P.J. (1993) Structural definition of the non-reducing termini of mannose-capped LAM from *Mycobacterium tuberculosis* through selective enzymatic degradation and fast atom bombardment-mass spectrometry. *Glycobiology* **3:** 497–506.

Dao, D.N., Kremer, L., Guerardel, Y., Molano, A., Jacobs, W.R., Jr, Porcelli, S.A., and Briken, V. (2004)

*Mycobacterium tuberculosis* lipomannan induces apoptosis and interleukin-12 production in macrophages. *Infect Immun* **72:** 2067–2074.

Davis, J.M., Clay, H., Lewis, J.L., Ghori, N., Herbomel, P., and Ramakrishnan, L. (2002) Real-time visualization of mycobacterium-macrophage interactions leading to initiation of granuloma formation in zebrafish embryos. *Immunity* **17:** 693–702.

Dinadayala, P., Kaur, D., Berg, S., Amin, A.G., Vissa, V.D., Chatterjee, D., *et al*. (2006) Genetic basis for the synthesis of the immunomodulatory mannose caps of lipoarabinomannan in *Mycobacterium tuberculosis*. *J Biol Chem* **281:** 20027–20035.

Dobson, G., Christie, W.W., and Nikolova-Damyanova, B. (1995) Silver ion chromatography of lipids and fatty acids. *J Chromatogr B Biomed Appl* **671:** 197–222.

Doz, E., Rose, S., Nigou, J., Gilleron, M., Puzo, G., Erard, F., *et al*. (2007) Acylation determines the toll-like receptor (TLR)-dependent positive versus TLR2-, mannose receptor-, and SIGNR1-independent negative regulation of pro-inflammatory cytokines by mycobacterial lipomannan. *J Biol Chem* **282:** 26014–26025.

Driessen, N.N., Stoop, E.J., Ummels, R., Gurcha, S.S., Mishra, A.K., Larrouy-Maumus, G., *et al*. (2010) Mycobacterium marinum MMAR_2380, a predicted transmembrane acyltransferase, is essential for the presence of the mannose cap on lipoarabinomannan. *Microbiology* **156:** 3492–3502.

Driessen, N.N., Boshoff, H.I., Maaskant, J.J., Gilissen, S.A., Vink, S., van der Sar, A.M., *et al*. (2012) Cyanovirin-N inhibits mannose-dependent mycobacterium-C-type lectin interactions but does not protect against murine tuberculosis. *J Immunol* **189:** 3585–3592.

Dye, C., Scheele, S., Dolin, P., Pathania, V., and Raviglione, M.C. (1999) Consensus statement. Global burden of tuberculosis: estimated incidence, prevalence, and mortality by country. WHO Global Surveillance and Monitoring Project. *JAMA* **282:** 677–686.

Festjens, N., Bogaert, P., Batni, A., Houthuys, E., Plets, E., Vanderschaeghe, D., *et al*. (2011) Disruption of the SapM locus in *Mycobacterium bovis* BCG improves its protective efficacy as a vaccine against *M. tuberculosis*. *EMBO Mol Med* **3:** 222–234.

Fratti, R.A., Chua, J., Vergne, I., and Deretic, V. (2003) *Mycobacterium tuberculosis* glycosylated phosphatidylinositol causes phagosome maturation arrest. *Proc Natl Acad Sci USA* **100:** 5437–5442.

Fukuda, T., Matsumura, T., Ato, M., Hamasaki, M., Nishiuchi, Y., Murakami, Y., *et al*. (2013) Critical roles for lipomannan and lipoarabinomannan in cell wall integrity of mycobacteria and pathogenesis of tuberculosis. *MBio* **4:** e00472-00412.

Geijtenbeek, T.B., Van Vliet, S.J., Koppel, E.A., Sanchez-Hernandez, M., Vandenbroucke-Grauls, C.M., Appelmelk, B., and Van Kooyk, Y. (2003) Mycobacteria target DC-SIGN to suppress dendritic cell function. *J Exp Med* **197:** 7–17.

Gilleron, M., Bala, L., Brando, T., Vercellone, A., and Puzo, G. (2000) *Mycobacterium tuberculosis* H37Rv parietal and cellular lipoarabinomannans. Characterization of the acyl- and glyco-forms. *J Biol Chem* **275:** 677–684.

Guerardel, Y., Maes, E., Elass, E., Leroy, Y., Timmerman, P., Besra, G.S., *et al*. (2002) Structural study of lipomannan and lipoarabinomannan from *Mycobacterium chelonae*. Presence of unusual components with alpha 1,3-mannopyranose side chains. *J Biol Chem* **277:** 30635–30648.

Guerardel, Y., Maes, E., Briken, V., Chirat, F., Leroy, Y., Locht, C., *et al*. (2003) Lipomannan and lipoarabinomannan from a clinical isolate of *Mycobacterium kansasii*: novel structural features and apoptosis-inducing properties. *J Biol Chem* **278:** 36637–36651.

Herbomel, P., Thisse, B., and Thisse, C. (2001) Zebrafish early macrophages colonize cephalic mesenchyme and developing brain, retina, and epidermis through a M-CSF receptor-dependent invasive process. *Dev Biol* **238:** 274–288.

Hmama, Z., Sendide, K., Talal, A., Garcia, R., Dobos, K., and Reiner, N.E. (2004) Quantitative analysis of phagolysosome fusion in intact cells: inhibition by mycobacterial lipoarabinomannan and rescue by an 1alpha,25-dihydroxyvitamin D3-phosphoinositide 3-kinase pathway. *J Cell Sci* **117:** 2131–2140.

Houben, D., Demangel, C., van Ingen, J., Perez, J., Baldeon, L., Abdallah, A.M., *et al*. (2012) ESX-1-mediated translocation to the cytosol controls virulence of mycobacteria. *Cell Microbiol* **14:** 1287–1298.

Jones, B.W., Means, T.K., Heldwein, K.A., Keen, M.A., Hill, P.J., Belisle, J.T., and Fenton, M.J. (2001) Different Toll-like receptor agonists induce distinct macrophage responses. *J Leukoc Biol* **69:** 1036–1044.

Kang, P.B., Azad, A.K., Torrelles, J.B., Kaufman, T.M., Beharka, A., Tibesar, E., *et al*. (2005) The human macrophage mannose receptor directs *Mycobacterium tuberculosis* lipoarabinomannan-mediated phagosome biogenesis. *J Exp Med* **202:** 987–999.

Karakousis, P.C., Bishai, W.R., and Dorman, S.E. (2004) *Mycobacterium tuberculosis* cell envelope lipids and the host immune response. *Cell Microbiol* **6:** 105–116.

Kaur, D., Berg, S., Dinadayala, P., Gicquel, B., Chatterjee, D., McNeil, M.R., *et al*. (2006) Biosynthesis of mycobacterial lipoarabinomannan: role of a branching mannosyltransferase. *Proc Natl Acad Sci USA* **103:** 13664–13669.

Kaur, D., Obregon-Henao, A., Pham, H., Chatterjee, D., Brennan, P.J., and Jackson, M. (2008) Lipoarabinomannan of Mycobacterium: mannose capping by a multifunctional terminal mannosyltransferase. *Proc Natl Acad Sci USA* **105:** 17973–17977.

Khoo, K.H., Dell, A., Morris, H.R., Brennan, P.J., and Chatterjee, D. (1995) Inositol phosphate capping of the nonreducing termini of lipoarabinomannan from rapidly growing strains of Mycobacterium. *J Biol Chem* **270:** 12380–12389.

Khoo, K.H., Tang, J.B., and Chatterjee, D. (2001) Variation in mannose-capped terminal arabinan motifs of lipoarabinomannans from clinical isolates of *Mycobacterium tuberculosis* and *Mycobacterium avium* complex. *J Biol Chem* **276:** 3863–3871.

Knutson, K.L., Hmama, Z., Herrera-Velit, P., Rochford, R., and Reiner, N.E. (1998) Lipoarabinomannan of *Mycobacterium tuberculosis* promotes protein tyrosine

dephosphorylation and inhibition of mitogen-activated protein kinase in human mononuclear phagocytes. Role of the Src homology 2 containing tyrosine phosphatase 1. *J Biol Chem* **273:** 645–652.

Kolk, A.H., Ho, M.L., Klatser, P.R., Eggelte, T.A., Kuijper, S., de Jonge, S., and van Leeuwen, J. (1984) Production and characterization of monoclonal antibodies to *Mycobacterium tuberculosis*, *M. bovis* (BCG) and *M. leprae*. *Clin Exp Immunol* **58:** 511–521.

Ludwiczak, P., Brando, T., Monsarrat, B., and Puzo, G. (2001) Structural characterization of *Mycobacterium tuberculosis* lipoarabinomannans by the combination of capillary electrophoresis and matrix-assisted laser desorption/ionization time-of-flight mass spectrometry. *Anal Chem* **73:** 2323–2330.

Ludwiczak, P., Gilleron, M., Bordat, Y., Martin, C., Gicquel, B., and Puzo, G. (2002) *Mycobacterium tuberculosis phoP* mutant: lipoarabinomannan molecular structure. *Microbiology* **148:** 3029–3037.

Lugo-Villarino, G., Balla, K.M., Stachura, D.L., Banuelos, K., Werneck, M.B., and Traver, D. (2010) Identification of dendritic antigen-presenting cells in the zebrafish. *Proc Natl Acad Sci USA* **107:** 15850–15855.

Maeda, N., Nigou, J., Herrmann, J.L., Jackson, M., Amara, A., Lagrange, P.H., *et al*. (2003) The cell surface receptor DC-SIGN discriminates between Mycobacterium species through selective recognition of the mannose caps on lipoarabinomannan. *J Biol Chem* **278:** 5513–5516.

Mishra, A.K., Driessen, N.N., Appelmelk, B.J., and Besra, G.S. (2011a) Lipoarabinomannan and related glycoconjugates: structure, biogenesis and role in *Mycobacterium tuberculosis* physiology and host-pathogen interaction. *FEMS Microbiol Rev* **35:** 1126–1157.

Mishra, A.K., Krumbach, K., Rittmann, D., Appelmelk, B., Pathak, V., Pathak, A.K., *et al*. (2011b) Lipoarabinomannan biosynthesis in Corynebacterineae: the interplay of two alpha(1–>2)-mannopyranosyltransferases MptC and MptD in mannan branching. *Mol Microbiol* **80:** 1241–1259.

Mishra, A.K., Alves, J.E., Krumbach, K., Nigou, J., Castro, A.G., Geurtsen, J., *et al*. (2012) Differential arabinan capping of lipoarabinomannan modulates innate immune responses and impacts T helper cell differentiation. *J Biol Chem* **287:** 44173–44183.

Nigou, J., Gilleron, M., Cahuzac, B., Bounery, J.D., Herold, M., Thurnher, M., and Puzo, G. (1997) The phosphatidylmyo-inositol anchor of the lipoarabinomannans from *Mycobacterium bovis* bacillus Calmette Guerin. Heterogeneity, structure, and role in the regulation of cytokine secretion. *J Biol Chem* **272:** 23094–23103.

Nigou, J., Gilleron, M., and Puzo, G. (1999) Lipoarabinomannans: characterization of the multiacylated forms of the phosphatidyl-myo-inositol anchor by NMR spectroscopy. *Biochem J* **337** (Part 3)**:** 453–460.

Nigou, J., Zelle-Rieser, C., Gilleron, M., Thurnher, M., and Puzo, G. (2001) Mannosylated lipoarabinomannans inhibit IL-12 production by human dendritic cells: evidence for a negative signal delivered through the mannose receptor. *J Immunol* **166:** 7477–7485.

Nigou, J., Gilleron, M., and Puzo, G. (2003) Lipoarabinomannans: from structure to biosynthesis. *Biochimie* **85:** 153–166.

Nigou, J., Vasselon, T., Ray, A., Constant, P., Gilleron, M., Besra, G.S., *et al*. (2008) Mannan chain length controls lipoglycans signaling via and binding to TLR2. *J Immunol* **180:** 6696–6702.

Pathak, S.K., Basu, S., Bhattacharyya, A., Pathak, S., Kundu, M., and Basu, J. (2005) *Mycobacterium tuberculosis* lipoarabinomannan-mediated IRAK-M induction negatively regulates Toll-like receptor-dependent interleukin-12 p40 production in macrophages. *J Biol Chem* **280:** 42794–42800.

Pitarque, S., Herrmann, J.L., Duteyrat, J.L., Jackson, M., Stewart, G.R., Lecointe, F., *et al*. (2005) Deciphering the molecular bases of *Mycobacterium tuberculosis* binding to the lectin DC-SIGN reveals an underestimated complexity. *Biochem J* **392:** 615–624.

Prouty, M.G., Correa, N.E., Barker, L.P., Jagadeeswaran, P., and Klose, K.E. (2003) Zebrafish-Mycobacterium marinum model for mycobacterial pathogenesis. *FEMS Microbiol Lett* **225:** 177–182.

Quesniaux, V.J., Nicolle, D.M., Torres, D., Kremer, L., Guerardel, Y., Nigou, J., *et al*. (2004) Toll-like receptor 2 (TLR2)-dependent-positive and TLR2-independent-negative regulation of proinflammatory cytokines by mycobacterial lipomannans. *J Immunol* **172:** 4425–4434.

Rajaram, M.V., Ni, B., Morris, J.D., Brooks, M.N., Carlson, T.K., Bakthavachalu, B., *et al*. (2011) *Mycobacterium tuberculosis* lipomannan blocks TNF biosynthesis by regulating macrophage MAPK-activated protein kinase 2 (MK2) and microRNA miR-125b. *Proc Natl Acad Sci USA* **108:** 17408–17413.

Ramakrishnan, L., Valdivia, R.H., McKerrow, J.H., and Falkow, S. (1997) *Mycobacterium marinum* causes both long-term subclinical infection and acute disease in the leopard frog (*Rana pipiens*). *Infect Immun* **65:** 767–773.

van der Sar, A.M., Musters, R.J., van Eeden, F.J., Appelmelk, B.J., Vandenbroucke-Grauls, C.M., and Bitter, W. (2003) Zebrafish embryos as a model host for the real time analysis of *Salmonella typhimurium* infections. *Cell Microbiol* **5:** 601–611.

van der Sar, A.M., Abdallah, A.M., Sparrius, M., Reinders, E., Vandenbroucke-Grauls, C.M., and Bitter, W. (2004) *Mycobacterium marinum* strains can be divided into two distinct types based on genetic diversity and virulence. *Infect Immun* **72:** 6306–6312.

Sena, C.B., Fukuda, T., Miyanagi, K., Matsumoto, S., Kobayashi, K., Murakami, Y., *et al*. (2010) Controlled expression of branch-forming mannosyltransferase is critical for mycobacterial lipoarabinomannan biosynthesis. *J Biol Chem* **285:** 13326–13336.

Sibley, L.D., Hunter, S.W., Brennan, P.J., and Krahenbuhl, J.L. (1988) Mycobacterial lipoarabinomannan inhibits gamma interferon-mediated activation of macrophages. *Infect Immun* **56:** 1232–1236.

Stamm, L.M., Morisaki, J.H., Gao, L.Y., Jeng, R.L., McDonald, K.L., Roth, R., *et al*. (2003) *Mycobacterium marinum* escapes from phagosomes and is propelled by actin-based motility. *J Exp Med* **198:** 1361–1368.

Stinear, T.P., Seemann, T., Harrison, P.F., Jenkin, G.A., Davies, J.K., Johnson, P.D., *et al*. (2008) Insights from the

complete genome sequence of *Mycobacterium marinum* on the evolution of *Mycobacterium tuberculosis*. *Genome Res* **18:** 729–741.

Stoop, E.J., Schipper, T., Huber, S.K., Nezhinsky, A.E., Verbeek, F.J., Gurcha, S.S., *et al*. (2011) Zebrafish embryo screen for mycobacterial genes involved in the initiation of granuloma formation reveals a newly identified ESX-1 component. *Dis Model Mech* **4:** 526–536.

Swaim, L.E., Connolly, L.E., Volkman, H.E., Humbert, O., Born, D.E., and Ramakrishnan, L. (2006) *Mycobacterium marinum* infection of adult zebrafish causes caseating granulomatous tuberculosis and is moderated by adaptive immunity. *Infect Immun* **74:** 6108–6117.

Tailleux, L., Schwartz, O., Herrmann, J.L., Pivert, E., Jackson, M., Amara, A., *et al*. (2003) DC-SIGN is the major *Mycobacterium tuberculosis* receptor on human dendritic cells. *J Exp Med* **197:** 121–127.

Talaat, A.M., Reimschuessel, R., Wasserman, S.S., and Trucksis, M. (1998) Goldfish, *Carassius auratus*, a novel animal model for the study of *Mycobacterium marinum* pathogenesis. *Infect Immun* **66:** 2938–2942.

Tatituri, R.V., Illarionov, P.A., Dover, L.G., Nigou, J., Gilleron, M., Hitchen, P., *et al*. (2007) Inactivation of *Corynebacterium glutamicum* NCgl0452 and the role of MgtA in the biosynthesis of a novel mannosylated glycolipid involved in lipomannan biosynthesis. *J Biol Chem* **282:** 4561–4572.

Torrelles, J.B., Azad, A.K., and Schlesinger, L.S. (2006) Fine discrimination in the recognition of individual species of phosphatidyl-myo-inositol mannosides from *Mycobacterium tuberculosis* by C-type lectin pattern recognition receptors. *J Immunol* **177:** 1805–1816.

Torrelles, J.B., Sieling, P.A., Arcos, J., Knaup, R., Bartling, C., Rajaram, M.V., *et al*. (2011) Structural differences in lipomannans from pathogenic and nonpathogenic mycobacteria that impact CD1b-restricted T cell responses. *J Biol Chem* **286:** 35438–35446.

Vergne, I., Chua, J., and Deretic, V. (2003) Tuberculosis toxin blocking phagosome maturation inhibits a novel Ca2+/calmodulin-PI3K hVPS34 cascade. *J Exp Med* **198:** 653–659.

Vignal, C., Guerardel, Y., Kremer, L., Masson, M., Legrand, D., Mazurier, J., and Elass, E. (2003) Lipomannans, but not lipoarabinomannans, purified from *Mycobacterium chelonae* and *Mycobacterium kansasii* induce TNF-alpha and IL-8 secretion by a CD14-toll-like receptor 2-dependent mechanism. *J Immunol* **171:** 2014–2023.

Volkman, H.E., Clay, H., Beery, D., Chang, J.C., Sherman, D.R., and Ramakrishnan, L. (2004) Tuberculous granuloma formation is enhanced by a mycobacterium virulence determinant. *PLoS Biol* **2:** e367.

van der Wel, N., Hava, D., Houben, D., Fluitsma, D., van Zon, M., Pierson, J., *et al*. (2007) *M. tuberculosis* and *M. leprae* translocate from the phagolysosome to the cytosol in myeloid cells. *Cell* **129:** 1287–1298.

Wittamer, V., Bertrand, J.Y., Gutschow, P.W., and Traver, D. (2011) Characterization of the mononuclear phagocyte system in zebrafish. *Blood* **117:** 7126–7135.

Wu, T., Guo, S., Wang, J., Li, L., Xu, L., Liu, P., *et al*. (2011) Interaction between mannosylated lipoarabinomannan and dendritic cell-specific intercellular adhesion molecule-3 grabbing nonintegrin influences dendritic cells maturation and T cell immunity. *Cell Immunol* **272:** 94–101.

## Supporting information

Additional Supporting Information may be found in the online version of this article at the publisher's web-site:

**Table S1.** Antibiotic susceptibility of *mptC* mutant.

**Fig. S1.** Schematic structure of lipoarabinomannan (LAM) of the different strains used in this study. Schematic representations of LAM of wildtype *M. marinum*, the *mptC* mutant, the capless mutant, the *mptC* mutant complemented with the *M. marinum* or *M. tuberculosis mptC* (*mptC* mutant + Mm/Mtb-*mptC*), or the *mptC* mutant complemented with the *M. smegmatis* mptC (*mptC* mutant + Msm-*mptC*). ManLAM is anchored into the mycobacterial cell envelope by its mannosylphosphatidyl-*myo*-inositol (MPI) moiety. The MPI anchor is linked to a mannan core consisting of $\alpha(1\rightarrow6)$-linked mannopyranose (man*p*) residues branched with $\alpha(1\rightarrow2)$-linked man*p* units. The structure is further glycosylated with an arabinan domain consisting of a linear $\alpha(1\rightarrow5)$-linked arabinofuranosyl (ara*f*) polymer branched with linear or bifurcating ara*f* side-chains. The non-reducing termini of the arabinan domain can be substituted with one to three man*p* residues; the mannose caps. The first man*p* unit is $\alpha(1\rightarrow5)$-linked and the following man*p* residues are $\alpha(1\rightarrow2)$-linked.

**Fig. S2.** $\alpha(1\rightarrow2)$-Mannosyltransferase activity of *mptC* mutant and related strains. *In vitro* $\alpha(1\rightarrow2)$-mannosyltransferase assay with synthetic nonasaccharide acceptor and membrane fractions from the blank (control), wildtype *M. marinum* (WT), *mptC* mutant (mptC), *mptC* mutant complemented with *mmar_3225* (mptC + *mptC* Mm), *mptC* mutant complemented with *msmeg4247* (mptC + *mptC* Msm) and *mptC* mutant complemented with *Rv2181* (mptC + *mptC* Mtb). The results represent mean + SEM of three independent experiments.

**Fig. S3.** Analysis of PIM biosynthesis in wildtype *M. marinum* (wildtype) and the *mptC* mutant (mptC). The polar lipids were extracted and examined by 2D-TLC. First and second dimensions are indicated by arrows and numbers.

**Fig. S4.** EM images of sections of THP-1 cells infected for 24 h with the *M. marinum mptC* mutant. Representative images of sections of cells with (A) cytosolic and (B) phagosomal *mptC* mutant bacterium (Mm), and immunogold labelled for CD63 with 10 nm gold particles, indicating the presence of phagosomal membranes. L, lysosome; M, mitochondria; N, nucleus; and the bars represent 200 nm.